Imaginary Cubes
— Objects with Three Square Projection Images —

Hideki Tsuiki

Graduate School of Human and Environmental Studies, Kyoto University
Kyoto, 606-8501, Japan E-mail: tsuiki@i.h.kyoto-u.ac.jp

May 23, 2009

1 Introduction.

Imagine a three dimensional object which has square projections in three orthogonal directions. A cube has this property, but it is not the only answer and there are plenty of examples like a regular tetrahedron and a cuboctahedron (Figure 1 (a) and (b)). Note that a regular tetrahedron looks square from one of its edges, and a cuboctahedron looks square from one of its square faces. A regular octahedron and a rhombic dodecahedron also have square projections in three orthogonal directions, but the inclinations of the three squares are different. Here, let us restrict our interest to the case that each pair of the three square shadow images has parallel edges, just like the shadow images of a cube. From an object with this property, one can imagine a cube which has the same three square projections. Therefore, we call such an object an *imaginary cube* (*I-cube* in short) and study them in detail. Figure 1 (c) and (d) are two important examples of polyhedral imaginary cubes; one has the form of a hexagonal bipyramid and the other one has the form of a triangular antiprismoid. They are explained in Section 3 and appear many times in this paper.
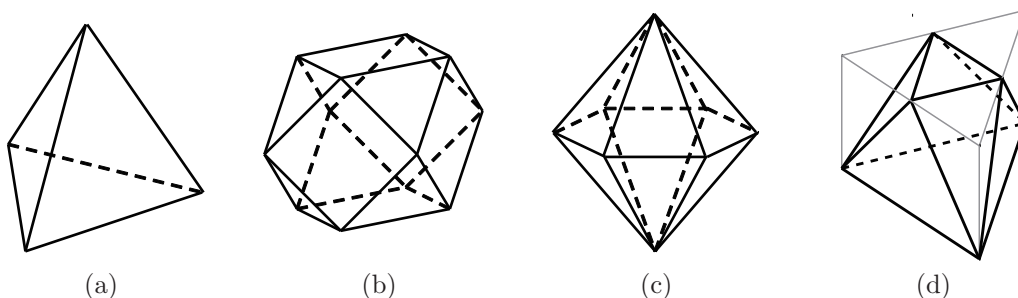

| (a) | (b) | (c) | (d) |

Figure 1: Examples of polyhedral imaginary cubes, (a) a regular tetrahedron, (b) a cuboctahedron, (c) a hexagonal bipyramid which has 12 isosceles triangle faces with the height 3/2 of a base, (d) a triangular antiprismoid obtained by truncating the vertices of one base of a regular triangular prism whose height is $\sqrt{6}/4$ of an edge of a base.

As well as polyhedral imaginary cubes, we study fractal imaginary cubes with the Hausdorff dimension two. Some fractal three-dimensional objects are attractive in that they have fractal shadow images which change smoothly as they are rotated three-dimensionally. A fractal imaginary cube is more attractive because the shadow image becomes a square in three orthogonal directions. Sierpinski tetrahedron is one example and we show many interesting examples of "two-dimensional" fractal imaginary cubes.

2   Minimal Convex Imaginary Cubes.

We say that an object is an *imaginary cube of a cube* (*I-cube of a cube* in short) if it produces the same three square projection images as the cube. We start with the problem of characterizing I-cubes of a given cube. First, if there is an I-cube of a cube, then its convex hull is also an I-cube of the same cube. Therefore, we only consider convex ones from which all the I-cubes are obtained by making some hollows without changing the three square projection images. Next, if a convex I-cube of a cube is given, then any convex object which is bigger than this object and contained in the cube is also a convex I-cube of the same cube. Therefore, we are particularly interested in minimal ones. In what follows, we study the problem of characterizing minimal convex I-cubes of a given cube.

Since we are studying convex objects, the three-square-projection property is equivalent to the property that the object is in the cube and has intersections with all the 12 edges of the cube. By minimality, it is the convex hull of its intersection with the cube-edges, which is a polyhedron. Therefore, our first observation is that a minimal convex I-cube of a cube is a polyhedron all of whose vertices are on cube-edges and each cube-edge contains at least one vertex. Suppose that two vertices are on the same cube-edge. If one of them is not a cube-vertex, then we can remove it to have a smaller I-cube. Therefore, our second observation is that if there are two vertices on one cube-edge, they should be the two endpoints of the cube-edge.

As the third observation, if the three adjacent cube-vertices of a cube-vertex v are vertices of a minimal convex I-cube, then v is not a vertex of the I-cube by minimality. On the other hand, if a set of cube-vertices which does not contain a vertex and its three adjacent vertices is given, then we can form a minimal convex I-cube of the cube by selecting one non-endpoint from each of the cube-edges whose endpoints are not in the set. Note that it is minimal because if we remove one vertex, then it no longer satisfies the first observation. Therefore, we can obtain all the minimal convex imaginary cubes of a cube in this way.

As Table 1 shows, there are 16 subsets of the set of cube-vertices which satisfy this condition if we identify rotationally congruent ones. Since No.10(L) and No.10(R) form a pair of mirror images and all the other ones have mirror symmetry, we have 15 subsets if we also identify reflectively congruent ones. We define that two minimal convex I-cubes of a cube are rotationally (or reflectively) equivalent if they have the same set of cube-vertices modulo rotational (or reflective) congruence. There are 16 (or 15) equivalent classes of minimal convex imaginary cubes of a given cube modulo rotational (or reflective) equivalence. This equivalence is natural in that when two equivalent minimal convex I-cubes of a cube are looked at from the same cube-surface, one can see the same kind of polygons connected in the same way by edges.

Now, we simply say that an object is a *minimal convex imaginary cube* if it is a minimal convex imaginary cube of some cube. Though some imaginary cubes are minimal convex imaginary cubes of two different cubes, such an imaginary cube is in the same equivalence class (No. 5) for both of the cubes, as we will explain in the next section. Therefore, we can say that there are 16 (or 15) equivalence classes of minimal convex imaginary cubes modulo rotational (or reflective) equivalence.

In Table 1, we list imaginary cubes obtained by taking middle points of cube-edges as non cube-vertices. This choice of the representatives of each equivalent class is natural in that, for almost all of the imaginary cubes in this list, the rotation group (or the full symmetry group) of an imaginary cube is equal to the group of rotations (or isometries) of the figure on the left which is a cube with some vertices colored. The only exception is No.5, which has a bigger group as we will explain in the next section. Among these imaginary cubes, No.10(L) and No.10(R) are mirror images and all the other ones have mirror symmetry. Note that all of the imaginary cubes in this list have rotational symmetry, even No.10(L) and No.10(R).
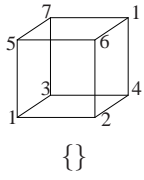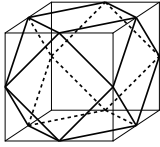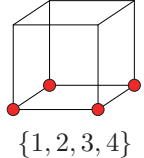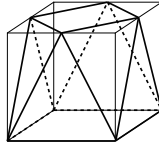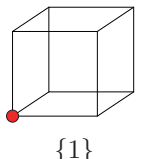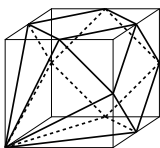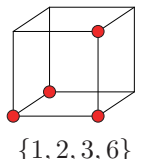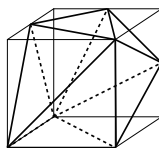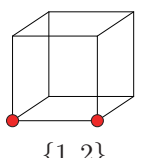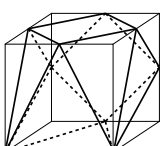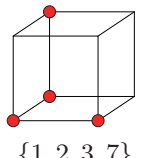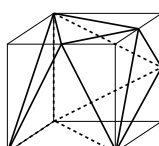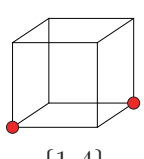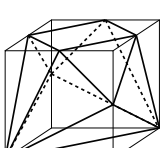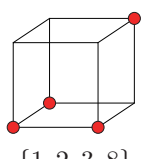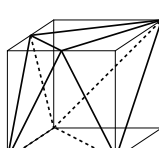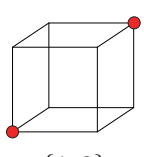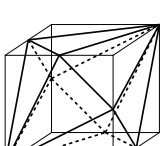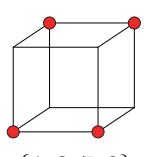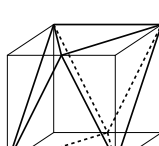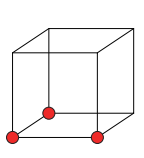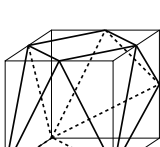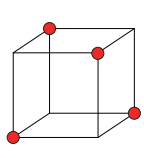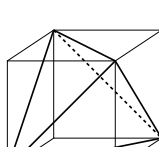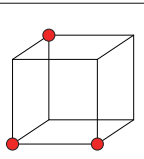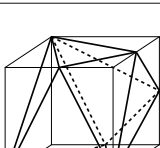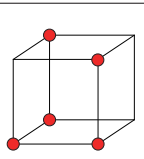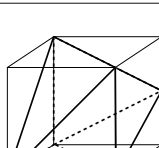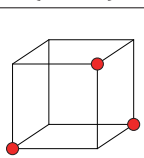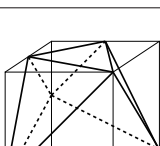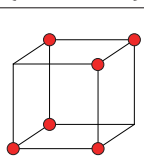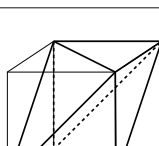
Number (#faces, #vertices)	Cube vertices	Imaginary cube			
1 (14,12) Cubocta-hedron	{}		9 (10,8) Quadric antiprismoid	{1, 2, 3, 4}	
2 (13,10)	{1}		10(L) (10,7)	{1, 2, 3, 6}	
3 (12,9)	{1, 2}		10(R) (10,7)	{1, 2, 3, 7}	
4 (11,8)	{1, 4}		11 (8,6)	{1, 2, 3, 8}	
5 (12,8) Hexagonal bipyramid	{1, 8}		12 (8,6)	{1, 2, 7, 8}	
6 (11,8)	{1, 2, 3}		13 (4,4) Regular tetrahedron	{1, 4, 6, 7}	
7 (10,6)	{1, 2, 7}		14 (8.6)	{1, 2, 3, 6, 7}	
8 (8,6) Triangular antiprismoid	{1, 4, 6}		15 (8,6) Triangular antiprism	{1, 2, 3, 6, 7, 8}	

Table 1: The 16 (or 15) representatives of minimal convex imaginary cubes.

3 Hexagonal Bipyramid and Triangular Antiprism Imaginary Cubes.

We explain more about some of the imaginary cubes in Table 1.

Regular tetrahedron (Table 1(13) , Figure 1(a)). As the figure in Table 1(13) shows, a regular tetrahedron is obtained by selecting as the vertices every other vertex of a cube. Therefore, it is an imaginary cube all of whose vertices are cube-vertices.

Cuboctahedron (Table 1(1) , Figure 1(b)). A cuboctahedron is an imaginary cube with no cube-vertices.

Triangular antiprism imaginary cube (Table 1(15)). A triangular antiprism with the sides right-angled isosceles triangles is an imaginary cube all of whose vertices are cube-vertices.

Hexagonal bipyramid imaginary cube (Table 1(5), Figure 1(c)). This dodecahedron is composed of two copies of a regular hexagonal pyramid whose side faces are isosceles triangles with the height 3/2 of the base. It has a square appearance when it is looked at from each of the 12 faces. We call an imaginary cube a *double imaginary cube* if it has square projections in 6 directions which are divided into two sets of three orthogonal directions. This dodecahedron is a double imaginary cube and the two cubes of which it is an imaginary cube share a pair of opposite vertices and one cube is obtained by rotating the other one by 60 degrees. Note that this double imaginary cube is the intersection of the two cubes. It means that it is a maximal double imaginary cube as well as a minimal one and therefore it is the only convex double imaginary cube of the two cubes. The rotation group of this imaginary cube is the dihedral group D_6 of order 12, which is not a subgroup of the rotation group of a cube; half of the rotations of this object map one cube to the other cube.

More generally, consider the intersection of two cubes which share a pair of opposite vertices. We have a dodecahedron which is a convex double imaginary cube of the two cubes as Figure 2(b) shows. One can easily show that all the convex double imaginary cubes are obtained in this way.

(a)   (b)
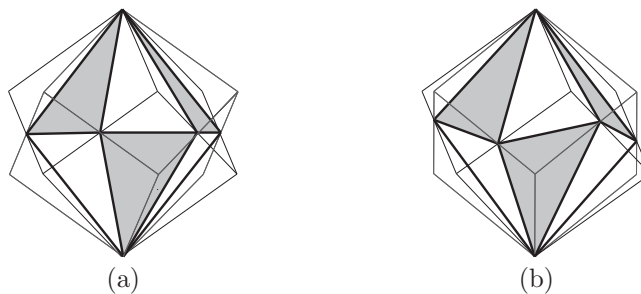
Figure 2: Double imaginary cubes obtained as the intersection of two cubes. One cube is obtained by rotating the other one by (a):60 degrees, (b): 42 degrees.

Triangular antiprismoid (Table 1(8), Figure 1(d)). Consider the polyhedron constructed from a regular n-sided prism by truncating each vertex of one base at middle points of the edges of the base and the adjoining vertex on the opposite base. We call the prismatoid constructed in this way an n-antiprismoid. Let us consider a triangular antiprismoid constructed from a regular triangular prism with the height $\sqrt{6}/4$ of an edge of a base. This octahedron is an imaginary cube as the figure in Table 1(8) shows, and has square appearances when looked at from the three thin isosceles triangular faces.

Figure 3 shows yet another property of this octahedron. It has the property that the three diagonals connecting two opposite vertices intersect at one point and are orthogonal to each other, and the crossing point divides each of the diagonals by the ratio of 1:2. Therefore, with some coordinate system, the six vertices are on the positive and the negative sides of

the three axes of coordinates and the distances from the origin to the three vertices on the negative sides are twice those to the vertices on the positive sides. Note that if all the six vertices have the same distance from the origin, then it is a regular octahedron.
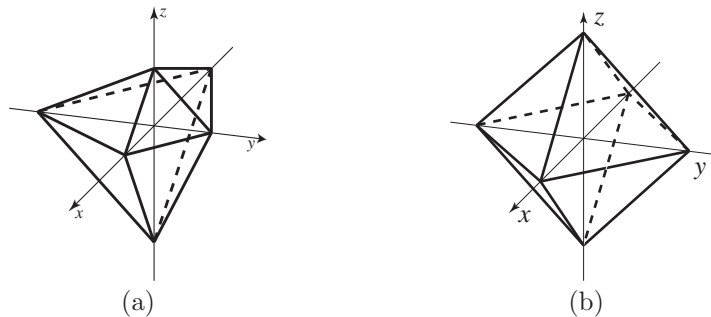
Figure 3: (a) Triangular antiprismoid imaginary cube and (b) regular octahedron.

Normally, it is not easy to realize at a glance that a given polyhedron is an imaginary cube. The author has an exhibition at Kyoto University Museum displaying models of imaginary cubes and asking guests to put them in a clear cubic box. It is not easy to put, for example, a regular tetrahedron into a box; people tend to pay attention to large triangular faces and try to fit them into a square, and it forms a good mathematical puzzle. Once an object is put into a box, one can realize that it is an imaginary cube by looking at it from the three surface directions of the box.

Figure 4: Imaginary cube puzzle.

4   Sierpinski Tetrahedron.

Sierpinski tetrahedron (Figure 5(a)) is a popular fractal realized in three-dimensional space. In fractal geometry, we say that an object is an IFS fractal (or a self-similar set) if it is the union of small copies of itself. Sierpinski tetrahedron is the union of four half-sized copies of itself and therefore it is an IFS fractal. As Figure 5(b) shows, it has square images when projected from its edges and therefore it is an imaginary cube.

We briefly introduce IFS fractals. Let F_i $(i = 1, \ldots, w)$ be similarity functions in the Euclidean space $\mathbb{R}^3$ with the ratios smaller than 1. We define the map $F(X) = \cup_{i=1}^{w} F_i(X)$ and apply it repeatedly to a non-empty compact subset C. Then, the sequence $C, F(C), F^2(C), \ldots$ converges with respect to the Hausdorff metric to a compact subset S not depending on the choice of C. The set S is called the IFS fractal generated by the iterated function system (IFS in short) $\{F_i\}_{(i=1,\ldots,w)}$. It satisfies $F(S) = S$ and S is the unique invariant of F among non-empty compact subset of $\mathbb{R}^3$. If all the similarity functions F_i $(i = 1, \ldots, w)$ have the same ratio $r < 1$ and the iterated function system satisfies the open set condition, that is, there is an open set O such that $F_i(O) \cap F_j(O) = \emptyset$ for all $i \neq j \leq w$, then, for C the closure of O, the sequence $C \supseteq F(C) \supseteq F^2(C) \supseteq \ldots$ is decreasing, the fractal S generated

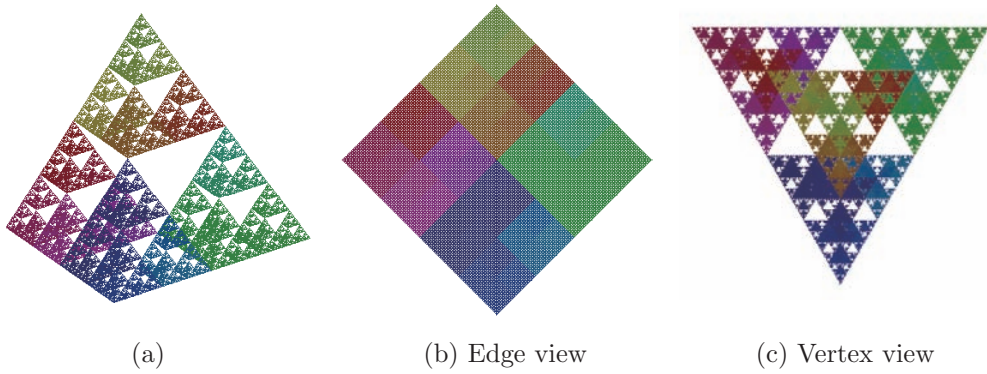<div align="center">(a)   (b) Edge view   (c) Vertex view</div>

Figure 5: Some projection images of the Sierpinski Tetrahedron.

by $\{F_i\}_{(i=1,\ldots,w)}$ is equal to the intersection $\cap_{i=0}^{\infty} F^i(C)$, and the Hausdorff dimension of S is $\log_{1/r}(w)$. We refer the reader to [2], [3], and [4] for the theory of fractals.

For the case of the Sierpinski tetrahedron, $w = 4$ and F_i are dilations (i.e., similarity functions which do not rotate the object) with the ratio $1/2$ and with the centers the four vertices of a regular tetrahedron A. It satisfies the open set condition for the interior of A. Therefore, we have a sequence $A = A_0 \supseteq A_1 \supseteq A_2 \supseteq \ldots$ of compact subsets of $\mathbb{R}^3$ by repeatedly applying the map F to A and $S = \cap_{i=0}^{\infty} A_i$ is the Sierpinski tetrahedron. In addition, it is two dimensional with respect to the Hausdorff dimension because $\log_2(4) = 2$.

<div align="center">$A_0 = A$ A_1 A_2 A_3 $\ldots$</div>
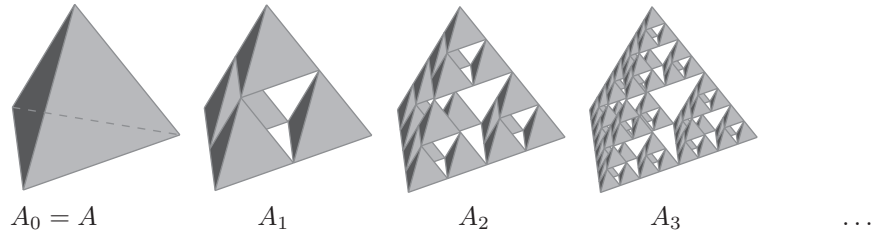
Figure 6: Approximations of the Sierpinski tetrahedron.

As we have seen, a regular tetrahedron A is an imaginary cube. We can show by induction that $A_k(k = 0, 1, 2, \ldots)$ are also imaginary cubes. Figure 7 is a sculpture which uses this fact. It has the shape of A_3 and is composed of 64 regular tetrahedron pieces, and two square pictures extended with the ratio $1 : \sqrt{3}$ are cut into 64 pieces and pasted on two faces of each tetrahedron. A picture can be seen from one edge and the other one from the opposite side.

Figure 7: Fractal University KYOTO. (Hideki Tsuiki, 2005).

From the fact that each A_i is an imaginary cube, one can show that the Sierpinski

<div align="center">6</div>

tetrahedron S is also an imaginary cube. Let $p : A \to E$ be one of the three square projections of the regular tetrahedron A to a square E. Fix a point y in E and let $D_i = p^{-1}(y) \cap A_i$ ($i = 0, 1, 2, \ldots$). We have $D_i \supset D_j$ for $i < j$ and each D_i is a non-empty compact subset. Therefore, their intersection, which is equal to $p^{-1}(y) \cap S$, is not empty. It means that some point of S is projected to y by p. Note that there is essentially no overlapping in this square projection in that $p^{-1}(y) \cap S$ is a one point set almost everywhere for $y \in E$.

5 Fractal Imaginary Cubes.

Now, we generalize Sierpinski tetrahedron and study fractal imaginary cubes. We study an imaginary cube S which is also an IFS fractal generated by an iterated function system with the following two properties.

(A) For some $k \geq 2$, it consists of k^2 similarity functions F_i ($i = 1, \ldots, k^2$) with the same ratio $1/k$.

(B) F_i ($i = 1, \ldots, k^2$) are dilations, that is, they do not make rotational transformations.

Let B be a cube of which S is an imaginary cube. From property (B), the k^2 similar copies $F_i(S)$ ($i = 1, \ldots, k^2$) have the same orientation as S. It ensures that the projection images are also IFS fractals. In particular, each square projection image is composed of k^2 squares of size $1/k$. From this fact, $F_i(B^\circ) \cap F_j(B^\circ) = \emptyset$ for B° the interior of the cube B and $i \neq j \leq k^2$, that is, this IFS satisfies the open set condition for B°. Therefore, for $F(X) = \cup_{i=1}^{k^2} F_i(X)$, the sequence $B \supset F(B) \supset F^2(B) \supset \ldots$ is decreasing and the fractal S is equal to the intersection $\cap_{i=0}^{\infty} F^i(B)$. It also shows that S has the Hausdorff dimension 2.

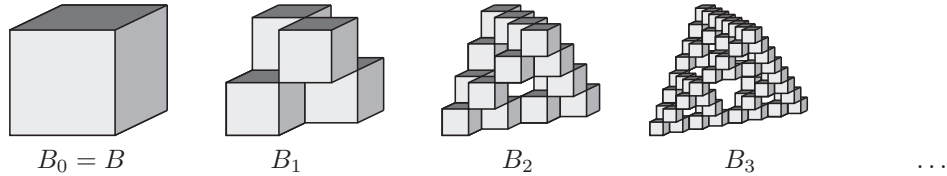$$B_0 = B \qquad B_1 \qquad B_2 \qquad B_3 \qquad \ldots$$

Figure 8: Cubic approximations of the Sierpinski tetrahedron.

Figure 8 shows the first three approximations of the Sierpinski tetrahedron starting with the cube B. Notice that this sequence and the sequence in Figure 6 converge to the same fractal object. The first approximation B_1 consists of four cubes which are selected from the 8 cubes obtained by dividing the cube B into $2 \times 2 \times 2$ and they are not overlapping in all the three surface-directions of B. Since B_{k+1} is obtained by substituting each cube of B_1 with B_k, this property of B_1 ensures by induction that each level of approximation is an imaginary cube.

For the general case, the first level cubic approximation $F(B)$ consists of k^2 small cubes $F_i(B)$ ($i = 1, \ldots, k^2$). Since $F(B)$ is contained in B and contains the imaginary cube S, it is also an imaginary cube. Therefore, the k^2 small cubes are obtained by dividing the cube B into $k \times k \times k$ small cubes and selecting k^2 of them so that they are not overlapping when viewed from the three surface directions. On the other hand, each selection of such k^2 cubes determines an IFS with properties (A) and (B), and as we explained for the case of Sierpinski tetrahedron, $F^i(B)$ ($i = 1, 2, \ldots$) are all imaginary cubes. From this fact, through the same arguments we had in the previous section, the limit is also an imaginary cube with the three square projections essentially non-overlapping. Therefore, we can conclude that all the fractal imaginary cubes generated by an IFS with properties (A) and (B) are obtained in this way.

By fixing one surface direction of such a configuration of k^2 small cubes, we have a $k \times k$ matrix of cubes with each of the cubes assigned a depth number from 1 to k. Therefore, we have a $k \times k$ matrix of integers in which each integer from 1 to k appears once in each

column and in each row. That is, it is a Latin square of size $k \times k$ [1]. Therefore, there is a one to one correspondence between such a configuration and a Latin square of size $k \times k$.

When $k = 2$, B_1 in Figure 8 is the only possible configuration if we identify those congruent through rotations of the cube, and the Sierpinski tetrahedron is the only fractal imaginary cube with properties (A) and (B). When $k = 3$, we have two rotationally non-congruent ways of selecting 9 cubes from the 27 cubes so that no overlapping occurs, which are **H** and **T** in Figure 9. In the following two sections, we study the fractals generated by them.
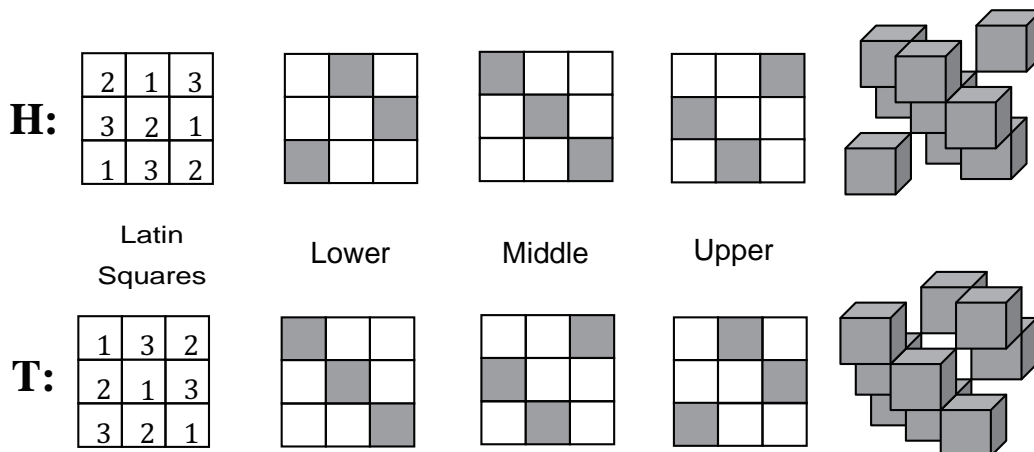

Figure 9: The two ways of selecting 9 cubes from 27 cubes so that no overlapping occurs in the three directions. **H** generates the hexagonal bipyramid fractal imaginary cube (Figure 10) and **T** generates the triangular antiprismoid fractal imaginary cube (Figure 12).
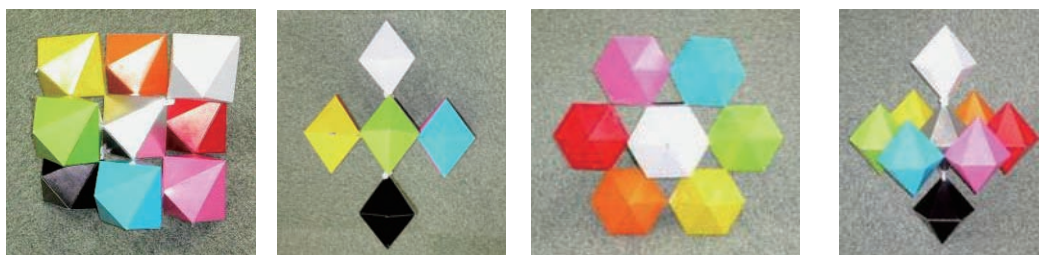
6 The Hexagonal Bipyramid Fractal.

In the lower part of Figure 10 are computer graphics images of the fractal generated by **H** projected in many directions. This fractal has 6-hold symmetry. Because of this symmetry, it has square projections (Figure 5 (d)) not in three but in **six** directions. That is, it is a fractal dual imaginary cube. It also has two kinds of "dendrites" ((e) and (h)), two kinds of "snowflakes" ((f) and (i)), and two kinds of tiling patterns ((g) and (j)). The structure of the tiling pattern (g) is investigated in [5]. Note that all the projection images are IFS fractals, as we noted in the previous section.

As we normally start not with a cube but with a regular tetrahedron to obtain a Sierpinski tetrahedron, it is more natural to start with the convex hull of the fractal to obtain its finite approximations. Since the similarity functions are dilations, the convex hull coincides with the convex hull of the centers of the dilations, which are the following nine points of the cube; (1) two opposite vertices, (2) six middle points of edges, and (3) the center. As the result, we have the hexagonal bipyramid imaginary cube in Table 1(5). We assembled models of level zero(i.e., hexagonal bipyramid imaginary cube) to level two approximations of this fractal with papers and piano wires (Figure 10 (a), (b), and (c)). Note that they are all double imaginary cubes.

The second level approximation model is composed of 81 pieces, and one can see a 9×9 matrix of squares when it has a square appearance. In the model of Figure 10(c), the pieces are colored with nine colors so that each of the nine rows, each of the nine columns, and each of the nine 3×3 blocks contains all the nine colors in each of the twelve square appearances. The author calls this coloring a 'Sudoku coloring' and showed that there are 30 Sudoku colorings of this second level approximation model if we identify congruent ones through reflections and change of colors [6]. The model of this picture has the most symmetric coloring among the 30 solutions. In Figure 11, this object is put in a clear 32-faced polygon with 12 square faces which are arranged so that it has square appearances from these faces. This sculpture is called the "fractal SUDOKU sculpture", and is displayed at Kyoto University Museum.
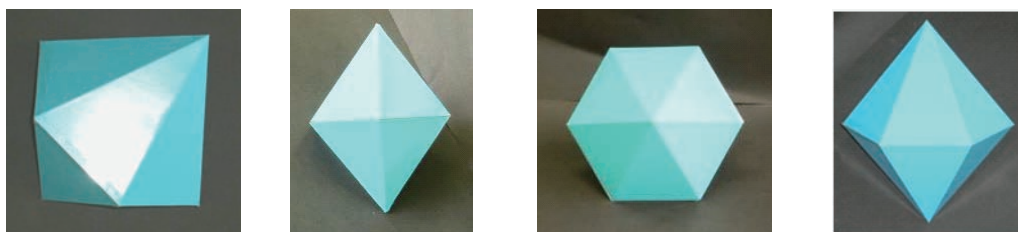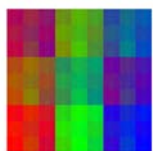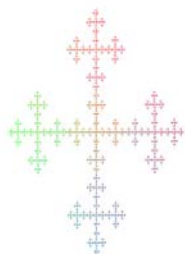
(a) Hexagonal bipyramid.

(b) First level approximation model.

(c) Second level approximation model with a SUDOKU coloring.
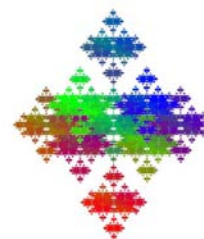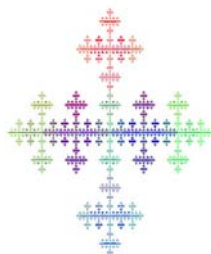

(d) Square (6)   (e) Dendrite #1 (3)   (f) Snowflake #1 (1)   (g) Tiling #1 (6)

(h) Dendrite #2 (3)   (i) Snowflake #2 (6)   (j) Tiling #2 (6)

Figure 10: The hexagonal bipyramid fractal and its finite approximation models viewed from many directions. In the parenthesis are the numbers of directions in which we have such projection images (opposite directions counted once).

Figure 11: The fractal SUDOKU sculpture (Hideki Tsuiki, 2006-2007).
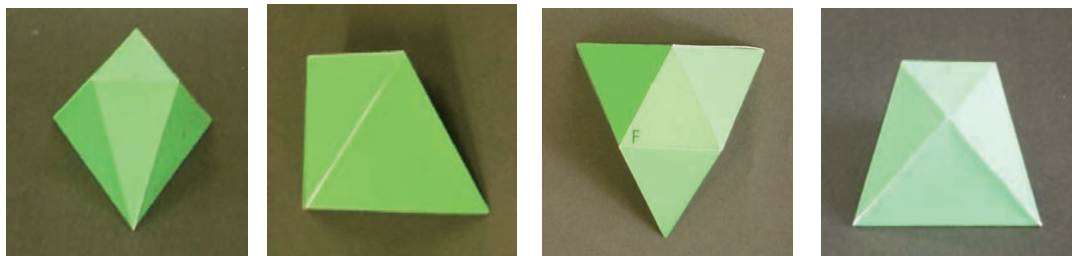
(a) Triangular antiprismoid.
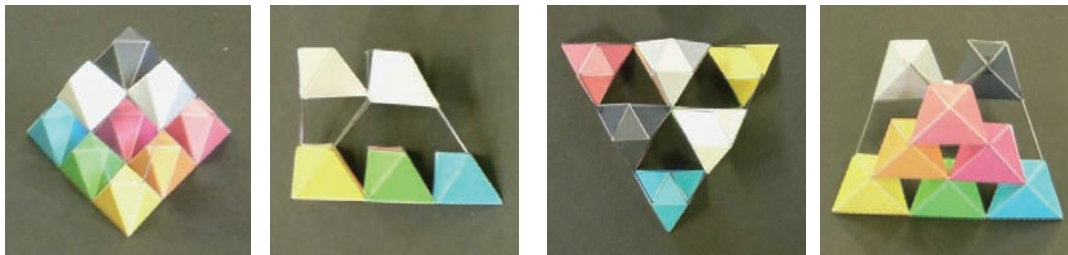
(b) First level approximation model.

(c) Square (3)   (d) Cantor Set #1 (3)   (e) Triangle (1)   (f) Tiling #1 (3)

(g) Cantor Set #2 (3)   (h) Tiling #2 (3)

Figure 12: The triangular antiprismoid fractal and its finite approximation models.

7 The Triangular Antiprismoid Fractal.

Figure 12 shows the fractal imaginary cube generated by the configuration **T**. In the lower part, there are projection images of this fractal from some directions. It has square projections in three orthogonal directions (Figure 12(c)). As (d) and (g) s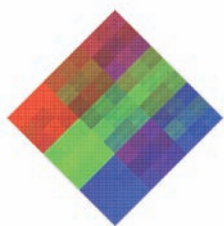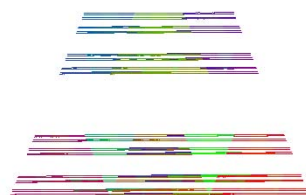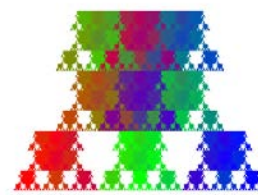how, this fractal is not connected. It is composed of slices which form the Cantor set. Figures (f) and (h) are fractal tiling patterns. The convex hull of this fractal is obtained by taking the convex hull of the centers of the dilations, which are the following points of the cube; (1) three vertices, (2) three midpoints of edges, and (3) three centers of faces. Here, the points in (3) are the middle points of the edges of the triangle generated from the points in (1), and thus can be omitted in taking the convex hull. We obtain, as the convex hull, a triangular antiprismoid imaginary cube in Table 1(8). Figure 12(a) is a model of a triangular antiprismoid imaginary cube, and Figure 12(b) is a model of the first level approximation.

8 The Case $k \geq 4$

The author wrote a program in Java to produce all the fractal imaginary cubes with properties (A) and (B) for $k \leq 5$. When $k = 4$, there are 36 reflectively non-congruent fractal imaginary cubes including the Sierpinski tetrahedron which already appeared for $k = 2$. One of them is shown in Figure 13, which is the only connected one except for the Sierpinski tetrahedron.

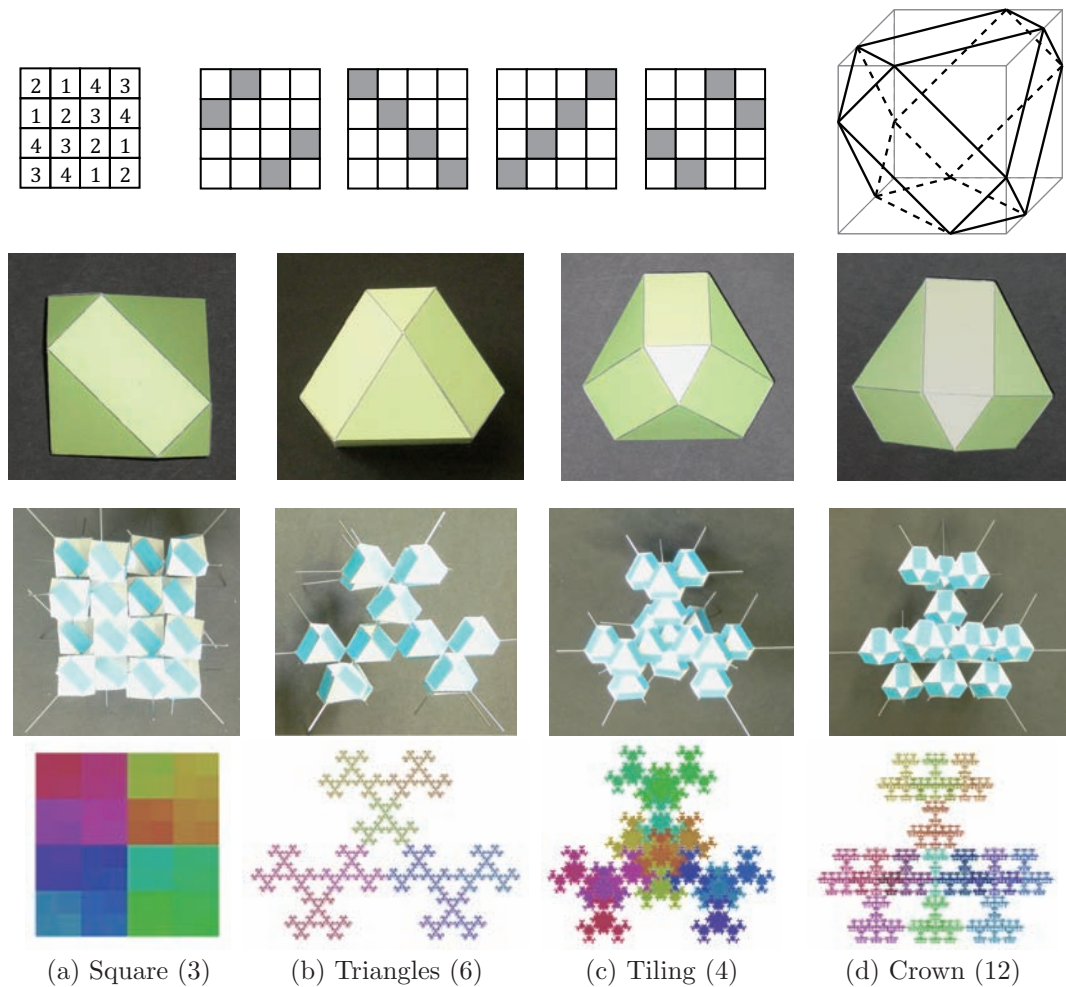(a) Square (3)　(b) Triangles (6)　(c) Tiling (4)　(d) Crown (12)

Figure 13: The non-Archimedean cuboctahedron fractal and its finite approximation models.

This fractal imaginary cube is also obtained through another IFS, which consists of 4 similarity maps with ratio 1/2 and 180 degrees rotations. Its convex hull is a non-Archimedean cuboctahedron with four of the triangular faces twice the size of the other four triangular faces. It is a minimal convex imaginary cube of the equivalence class Table 1(1). When k is equal to 5, we have 3482 solutions. There is a Java applet in the author's homepage which displays all the fractal imaginary cubes up to $k \leq 5$ [7].

As the number k increases, the number of fractal imaginary cubes obtained in this way increases explosively. Among them, there is a series of fractals. Recall the configuration for the antiprismoid fractal imaginary cube in Figure 9(T). The lower level is a diagonal sequence of cubes, and the middle level is its shift to the right with the overflowed one appearing from the left. This construction of a configuration applies to every k, as the following figure shows.
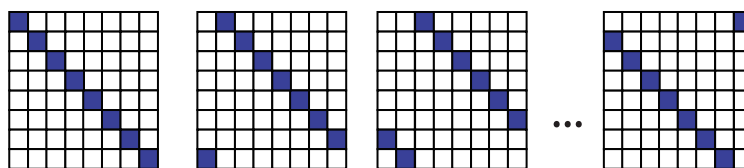

Figure 14: A series of configurations whose fractals converge to two sheets of triangles.

Correspondingly, we have a sequence of fractal imaginary cubes. This sequence converges with respect to the Hausdorff metric and, as the limit, we obtain a simple shape in Figure 15 which consists of two triangular sheets. Though this limit is not an IFS fractal, it is an imaginary cube. Note that it is the two bases of the triangular antiprism imaginary cube (Table 1(15)). The object in Figure 15 is a simple application of this shape. In this sculpture, two triangular sheets have drawings and the cube is made of acrylic glass. One can see from three faces of the cube the three rhombic images obtained by connecting the two drawings affine-transformed to squares.
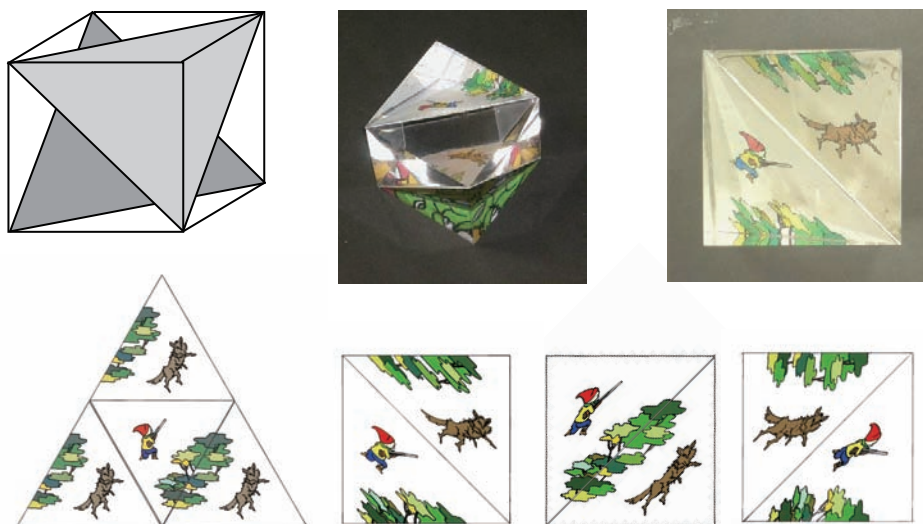

Figure 15: A Boy and a Wolf (Hideki Tsuiki and Yumiko Ihara, 2007).

9 A 3D Tiling with Hexagonal Bipyramids and Triangular Antiprismoids.

Hexagonal bipyramid imaginary cubes and triangular antiprismoid imaginary cubes form a tiling of three-dimensional space as Figure 16 shows. The ratio of bipyramids to antiprismoids in this tessellation is 1 to 4. In this picture, bipyramids have blue (dark) color and antiprismoids have four colors.
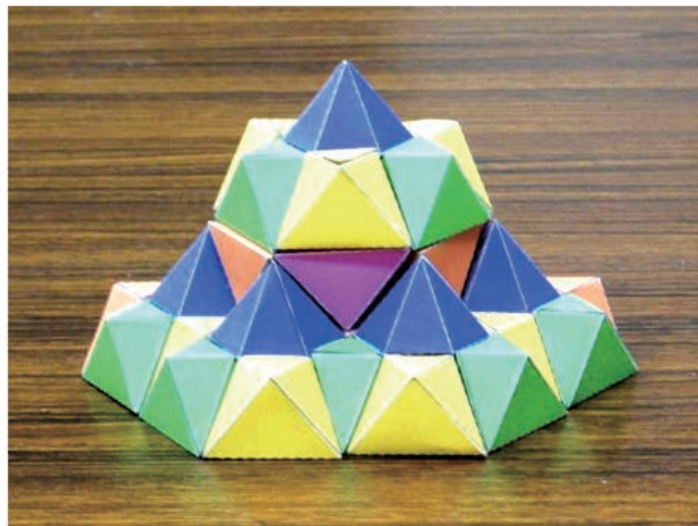

Figure 16: The 3D tiling with hexagonal bipyramids and triangular antiprismoids.

Before studying this tiling, we explain the well-known tiling of three-dimensional space by regular tetrahedrons and regular octahedrons. We call the cube B in Figure 8 a large cube and each component cube of the first level cubic approximation B_1 a small cube. Comparing the two first level approximations A_1 and B_1 of the Sierpinski tetrahedron, one can see that A_1 is obtained by replacing the four cubes of B_1 with regular tetrahedrons. Since two copies of B_1 fill the large cube B, by replacing these two copies of B_1 with A_1, one obtains in B eight regular tetrahedrons and a void space left around the small-cube vertex at the center. Since the eight regular tetrahedrons share vertices at the centers of the six surfaces of the large cube, the void space has the form of a regular octahedron. Now, consider the infinite lattice of cubes which are tiling three-dimensional space and apply the same construction considering each cube as a large cube. This time, we have void spaces left also at the small-cube vertices which are middle points of the large-cube edges, and they are also regular octahedrons. Thus, we obtain the three-dimensional tiling with regular tetrahedrons and regular octahedrons.

For the case of antiprismoids and bipyramids, we consider, in addition to the configurations in Figure 9, the following configuration which is a rotation of configuration **T** and thus also produces the antiprismoid fractal imaginary cube with a different orientation.
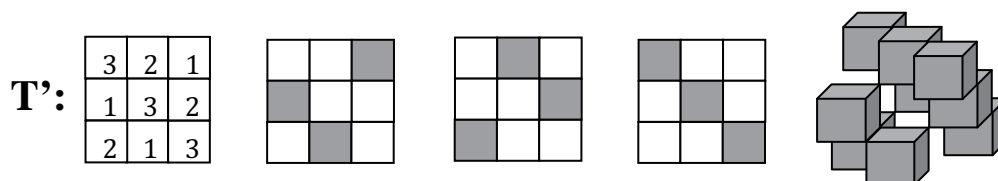

Figure 17: Another configuration which generates the antiprismoid fractal.

The three configurations **H**, **T**, and **T**′ are not overlapping and they fill a large cube. Now, we replace them with the first level approximations of the corresponding fractals. In this way, the large cube contains 9 bipyramids, 9 antiprismoids, and 9 antiprismoids with another orientation. In addition, there are 8 small-cube vertices inside the large cube, and two of them are occupied and therefore we have void spaces around 6 small-cube vertices. Each bipyramid and antiprismoid has one vertex on each edge of the small cube in which it is contained, and one can see that these 27 polyhedra share vertices on each shared edge of the surrounding cubes. Thus, the void spaces left in the large cube are octahedrons surrounded by the two kinds of polyhedra in the surrounding 8 small cubes. One can see that they are antiprismoids, because each of the octahedrons has three of the vertices located on small-cube vertices and the other three on middle points of small-cube edges. Recall the remarkable property of an antiprismoid in Figure 3. Thus, we can fill the voids in the cube with six antiprismoids. This procedure can be generalized to the tiling of three-dimensional space with cubes, and as the result, we obtain a tiling of three-dimensional space with bipyramids and antiprismoids.

Finally, we explain that this three-dimensional tiling is a Voronoi tessellation. A Voronoi tessellation is defined for a set V of points with no accumulation points. For $v \in V$, consider the set of points which are closer to v than to any other points of V and take its closure to form a polyhedron $P(v)$. Then, $\{P(v) \mid v \in V\}$ form a tiling, which is called the Voronoi tessellation corresponding to the set V. Many three-dimensional tilings are explained as Voronoi tessellations, for example, a cubic lattice generates a tessellation with cubes, a face-centered cubic lattice generates a tessellation with rhombic dodecahedrons, and a body-centred cubic lattice generates a tessellation with truncated octahedra.

Now, we study the set of points which generates our three-dimensional tessellation with bipyramids and antiprismoids. We define the center of an antiprismoid as the center of the cube containing it. We consider the cubic lattice X of points with three integer coordinates. For the sublattice of points with the three coordinates multiples of 3, take the Voronoi tessellation to form a tessellation of cubes and apply the procedure explained above. Then, we have the Voronoi tessellation of X each of whose component cubes contains one of a bipyramid or an antiprismoid. Here, the centers of the bipyramids are located on planes $x + y + z = 3k$ for k integers, and those of antiprismoids coming from the configuration **T** and **T**′ are located on planes $x + y + z = 3k + 1$ and $x + y + z = 3k - 1$, respectively as Figure 18(a) shows. On each of these three kinds of planes, lattice points of X form an equilateral triangular lattice. Figure 18(b) shows parts of these lattices projected along the line $x = y = z$. As this figure shows, the three kinds of planes are projected to different equilateral triangular lattices.
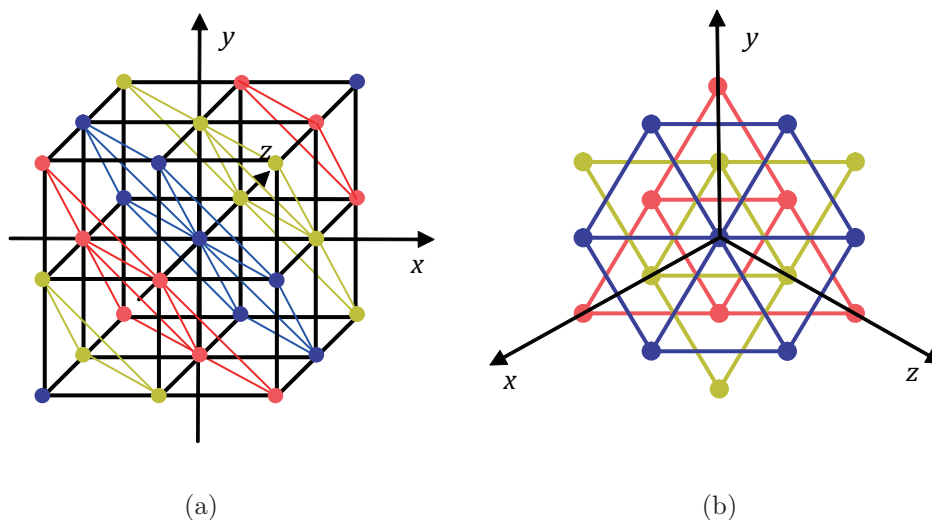

(a)   (b)

Figure 18: The relation between (a) a cubic 3D lattice and (b) equilateral triangle lattices.

Let Y be the cubic lattice obtained by rotating X around the axis $x = y = z$ by 60 degrees. Since our three-dimensional tiling with bipyramids and antiprismoids has order 6 (60 degrees) rotational symmetry around this axis, centers of bipyramids and antiprismoids exist also on the lattice Y. The intersection of the two lattices X and Y is the union of the triangle lattices corresponding to $x + y + z = 3k$ for k integers, that is, the centers of the bipyramids. Therefore, in this tiling, centers of the bipyramids are located on $X \cap Y$ and the centers of antiprismoids are located on $X \cup Y \setminus X \cap Y$. The distance between a center of a bipyramid and that of an adjacent antiprismoid is 1, whereas the distances from these centers to the face between them are $1/2$. It is obvious that for two adjacent antiprismoids, the face between them perpendicularly bisects the line segment between their centers. Therefore, we can conclude that the tiling with bipyramids and antiprismoids is a Voronoi tessellation of the union of a cubic lattice and its 60 degree rotation.

Acknowledgements.

References

[1] J. Denes and A. D. Keedwell, *Latin Squares and their Applications*, Academic Press, New York, 1974.

[2] G. A. Edgar, *Measure Topology and Fractal Geometry*, Springer-Verlag, 1990.

[3] K. J. Falconer, *Fractal Geometry - Mathematical Foundations and Applications*, John Wiley, 1990.

[4] J. E. Hutchinson, Fractals and self similarity, *Indiana Univ. Math. J.* 30, pp.713-747, 1981.

[5] H. Tsuiki, Does it Look Square? -Hexagonal Bipyramids, Triangular Antiprismoids, and their Fractals, *in: Sarhagi, R., Barrallo, J. (eds.) Proceedings of Conference Bridges Donostia - Mathematical Connections in Art, Music, and Science*, pp. 277-286, Tarquin publications, 2007.

[6] H. Tsuiki, SUDOKU Colorings of the Hexagonal Bipyramid Fractal, *in: Ito et al. (eds.) Computational Geometry and Graph Theory, Lecture Notes in Computer Science Vol. 4535*, pp. 224-235, Springer Berlin/Heidelberg, 2008.

[7] H. Tsuiki, A webpage on Imaginary Cubes.
    http://www.i.h.kyoto-u.ac.jp/~tsuiki/index-e.html.